

IL-23/IL-17A/TRPV1 Axis Produces Mechanical Pain via Macrophage-Sensory Neuron Crosstalk in Female Mice

Xin Luo, Ouyang Chen, Zilong Wang, Sangsu Bang, Jasmine Ji, Sang Hoon Lee, Yul Huh, Kenta Furutani, Qianru He, Xueshu Tao, Mei-Chuan Ko, Andrey Bortsov, Christopher R Donnelly, Yong Chen, Andrea Nackley, Temugin Berta, and Ru-Rong Ji

Supplemental Information (items)

I. Supplemental Figures (8)

Figure S1 (related to Figure 1)

Figure S2 (related to Figure 2)

Figure S3 (related to Figure 3)

Figure S4 (related to Figure 4)

Figure S5 (related to Figure 5)

Figure S6 (related to Figure 6)

Figure S7 (related to Figure 7)

Figure S8 (related to Figure 8)

II. Supplemental Tables

Table S1 (related to Figure 4 and Figure 5): Gating strategy of flow cytometry

Table S2 (related to Figure 8): qPCR primer sequences for human genes

Table S3 (related to all figures): Number of animals used in all figures in the paper

Table S4 (related to all figures): Statistical details of all figures in the paper (separate Excel file)

Table S5 (related to all figures): Source data for figures in the paper (separate Excel file)

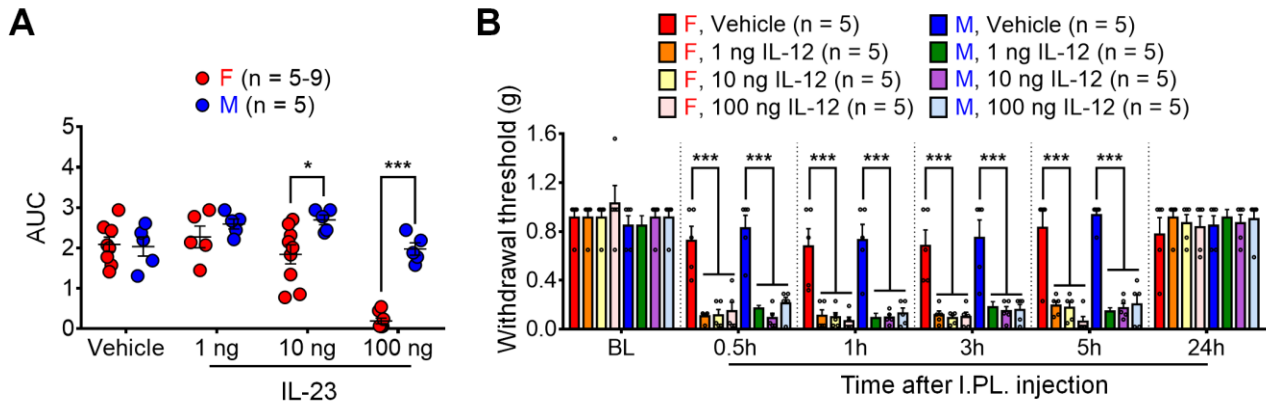


Figure S1 (related to Figure 1). IL-23, but not IL-12, exhibits sex difference in producing mechanical pain in mice.

(A) AUC of 0.5-5 h data in Fig. 1A shows that IL-23 at 10 ng and 100 ng induces female-dominant mechanical pain. * $p < 0.05$, *** $p < 0.001$. Two-way ordinary ANOVA with Bonferroni's post hoc test: $F_{(3, 42)} = 8.274$.

(B) I.PL. injection of IL-12 at 1 ng, 10 ng or 100 ng induces comparable mechanical allodynia in both sexes. *** $p < 0.001$. Two-way RM ANOVA with Bonferroni's post hoc test: $F_{(35, 160)} = 5.533$.

Data are mean \pm SEM. AUC: Area under curve; I.PL.: Intraplantar; BL: Baseline.

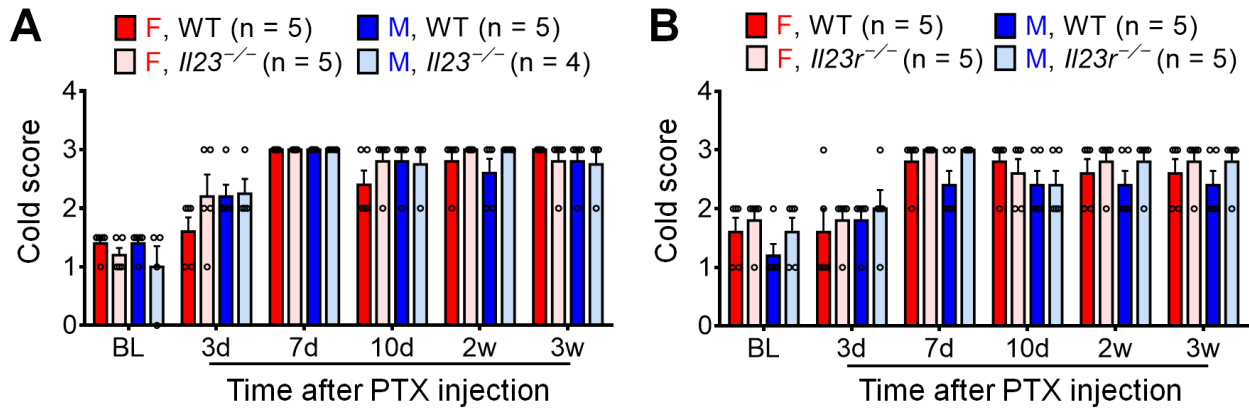


Figure S2 (related to Figure 2). IL-23/IL-23R axis does not mediate cold pain in the CIPN model.

Loss of IL-23 (*Il23*^{-/-}, A) or IL-23 receptor (*Il23r*^{-/-}, B) fails to alter cold allodynia in neither female nor male mice in the CIPN model (1 x PTX, 6 mg/kg). Two-way RM ANOVA with Bonferroni's post hoc test; A: $F_{(15, 75)} = 1.365$; B: $F_{(15, 80)} = 0.4865$.

Data are mean \pm SEM. PTX: Paclitaxel; BL: Baseline.

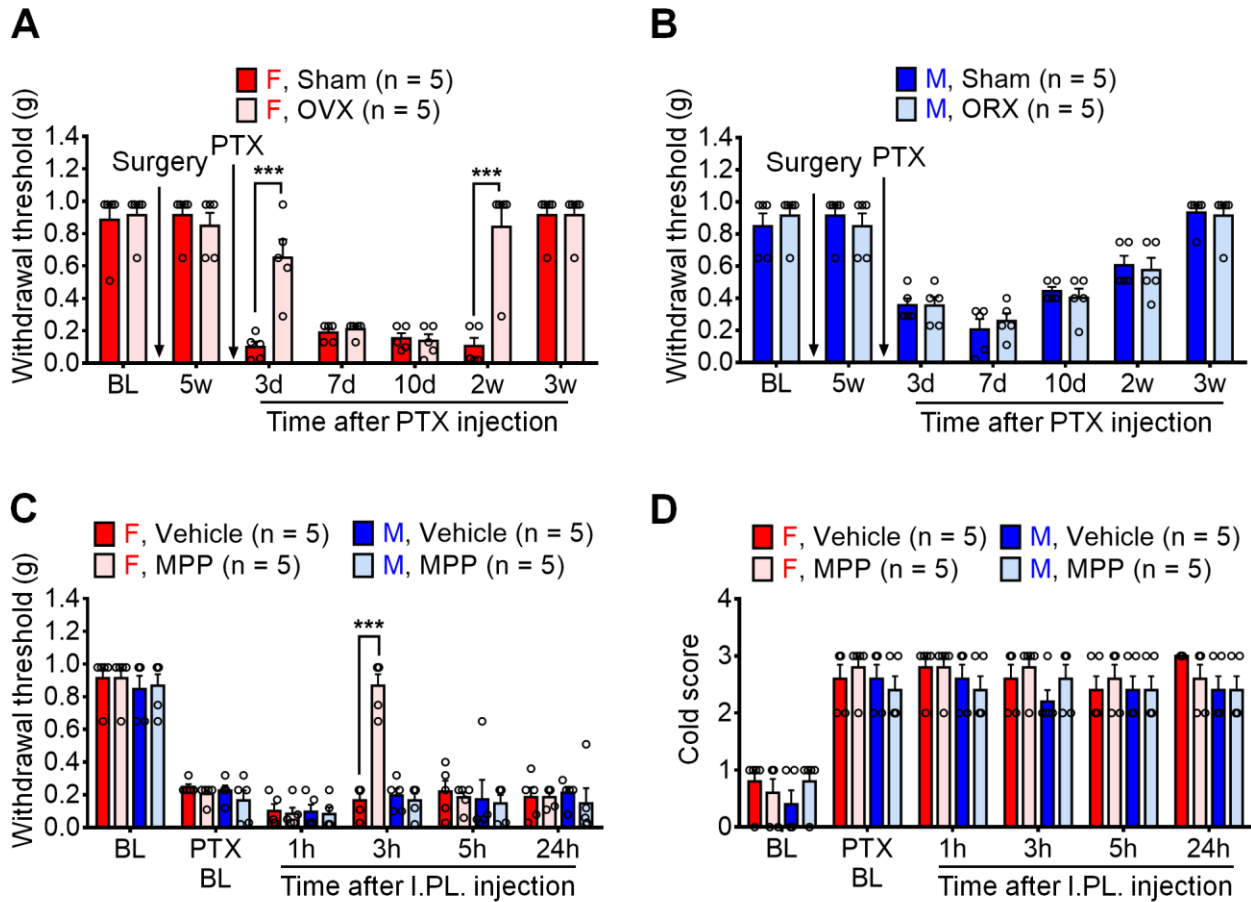


Figure S3 (related to Figure 3). Estrogen/ER α signaling contributes to pathological pain only in female mice.

(A) Estrogen deficiency by OVX reduces mechanical allodynia in females at 3d and 2w in CIPN (1 x PTX, 6 mg/kg). *** $p < 0.001$. Two-way RM ANOVA with Bonferroni's post hoc test; $F_{(6, 48)} = 11.08$.

(B) Androgen deficiency by ORX does not affect mechanical allodynia in males in CIPN (1 x PTX, 6 mg/kg). Two-way RM ANOVA with Bonferroni's post hoc test; $F_{(6, 48)} = 0.4182$.

(C) Estrogen receptor α antagonist MPP (I.PL., 30 μ g) reduces mechanical allodynia in female but not male mice in CIPN (4 x PTX, 2 mg/kg). *** $p < 0.001$. Two-way RM ANOVA with Bonferroni's post hoc test; $F_{(15, 80)} = 7.068$.

(D) MPP (I.PL., 30 μ g) fails to affect cold allodynia in CIPN (4 x PTX, 2 mg/kg). Two-way RM ANOVA with Bonferroni's post hoc test; $F_{(15, 80)} = 0.5895$.

Data are mean \pm SEM. OVX: Ovariectomy; ORX: Orchiectomy; I.PL.: Intraplantar; PTX: Paclitaxel; BL: Baseline.

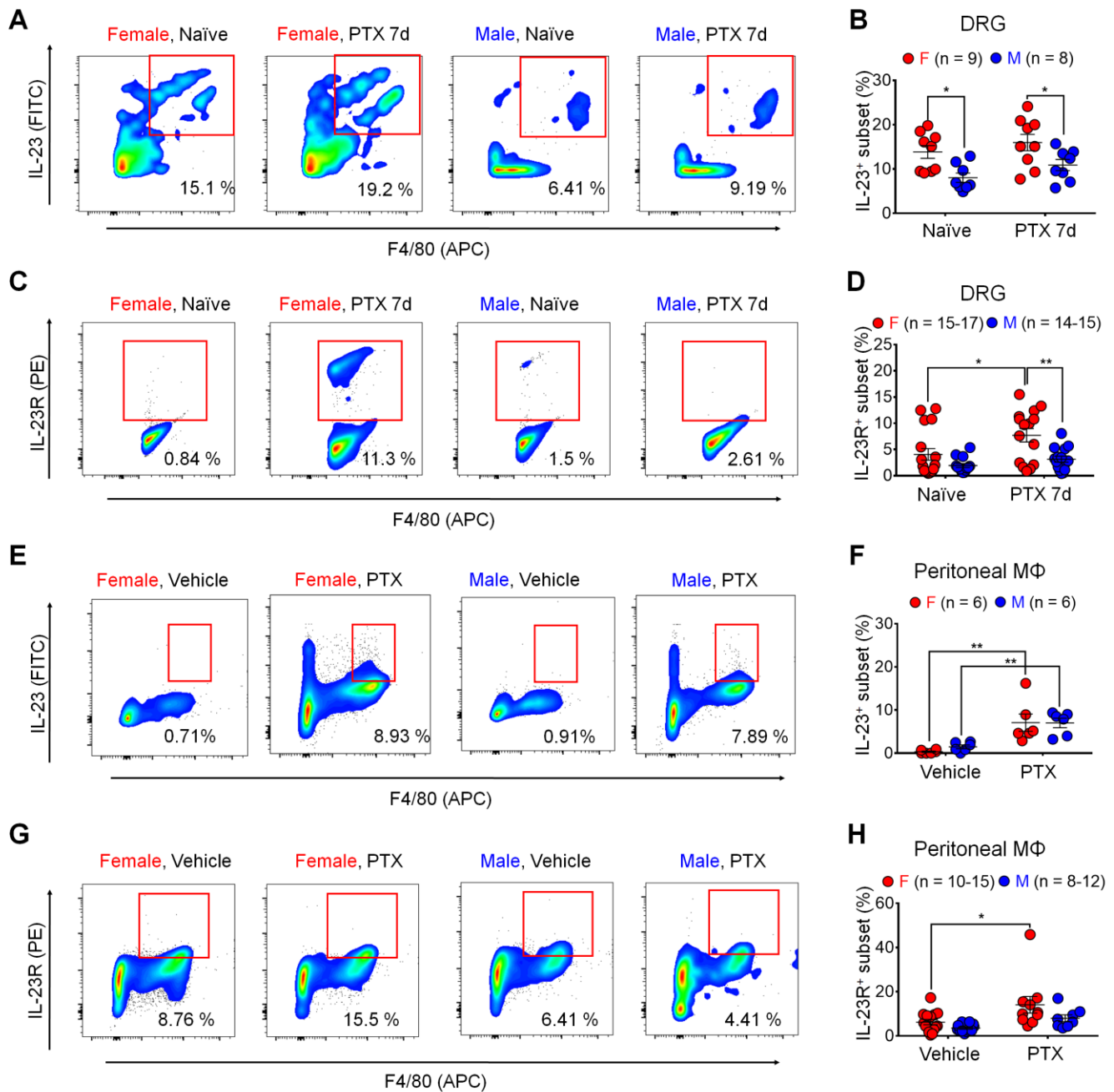


Figure S4 (related to Figure 4). Females exhibit higher levels of IL-23⁺ and IL-23R⁺ subsets in peritoneal and DRG macrophages than males under chemotherapy condition.

(A-B) Females display higher ratios of IL-23⁺ subset in DRG macrophages than males under naïve and chemotherapy conditions (4 x PTX, 2 mg/kg). (A) Images of flow cytometry. (B) Quantification of IL-23⁺ subset of DRG cells. *p < 0.05. Two-way ordinary ANOVA with Bonferroni's post hoc test; $F_{(1, 30)} = 0.06378$.

(C-D) PTX increases ratios of IL-23R⁺ subset in DRG macrophages from female but not male mice (4 x, 2 mg/kg). (C) Images of flow cytometry. (D) Quantification of IL-23R⁺ subset of DRG cells. *p < 0.05, **p < 0.01. Two-way ordinary ANOVA with Bonferroni's post hoc test; $F_{(1, 57)} = 1.682$.

(E-F) PTX increases ratios of IL-23⁺ subset in peritoneal macrophages cultured from both female and male mice (1 µg/ml, 16 h). (E) Images of flow cytometry. (F) Quantification of IL-23⁺ peritoneal macrophages. **p < 0.01. Two-way ordinary ANOVA with Bonferroni's post hoc test: $F_{(1, 20)} = 0.2641$.

(G-H) PTX increases ratios of IL-23R⁺ subset in peritoneal macrophages cultured from female not male mice (1 µg/ml, 16 h). (G) Images of flow cytometry. (H) Quantification of IL-23R⁺ peritoneal macrophages. *p < 0.05.

Two-way ordinary ANOVA with Bonferroni's post hoc test, $F_{(1, 41)} = 0.7265$.

Data are mean \pm SEM. PTX: Paclitaxel; M Φ : Macrophage.

See Table S1 for the gating strategy of flow cytometry.

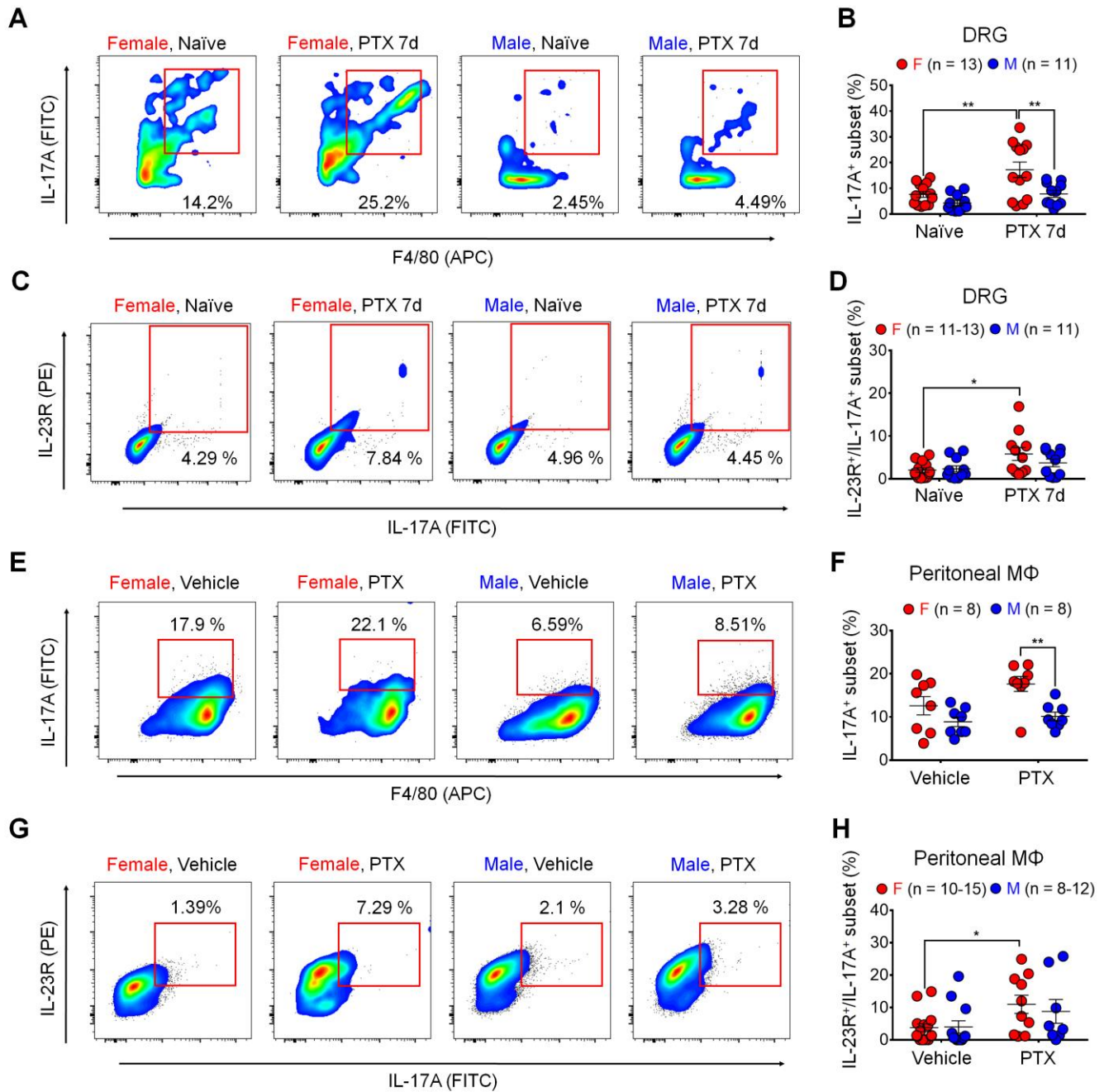


Figure S5 (related to Figure 5). PTX increases IL-17A⁺ and IL-17A⁺/IL-23R⁺ subsets in DRG and peritoneal macrophages.

(A-B) PTX increases ratios of IL-17A⁺ subset in DRG macrophages from female but not male mice (4 x PTX, 2 mg/kg). (A) Images of flow cytometry. (B) Quantification of IL-17A⁺ subset of DRG cells. **p < 0.01. Two-way ordinary ANOVA with Bonferroni's post hoc test; $F_{(1,44)} = 2.531$.

(C-D) PTX increases ratios of IL-17A⁺/IL-23R⁺ subset in DRG macrophages from female but not male mice (4 x, 2 mg/kg). (C) Images of flow cytometry. (D) Quantification of IL-17A⁺/IL-23R⁺ subset of DRG cells. *p < 0.05. Two-way ordinary ANOVA with Bonferroni's post hoc test: $F_{(1,42)} = 1.529$.

(E-F) PTX increases ratios of IL-17A⁺ subset in peritoneal macrophages from female but not male mice (1 μg/ml, 16 h). (E) Images of flow cytometry. (F) Quantification of IL-17A⁺ subset of peritoneal macrophages. **p < 0.01. Two-way ordinary ANOVA with Bonferroni's post hoc test, $F_{(1,28)} = 1.487$.

(G-H) PTX increases ratios of IL-17A⁺/IL-23R⁺ subset in female peritoneal macrophages (1 μg/ml, 16h). *p <

0.05. (G) Images of flow cytometry. (H) Quantification of IL-17A⁺/IL-23R⁺ subset of peritoneal macrophages. Two-way ordinary ANOVA with Bonferroni's post hoc test; $F_{(1, 41)} = 0.2854$.

Data are mean \pm SEM. PTX: Paclitaxel; M Φ : Macrophage.

See Table S1 for the gating strategy of flow cytometry.

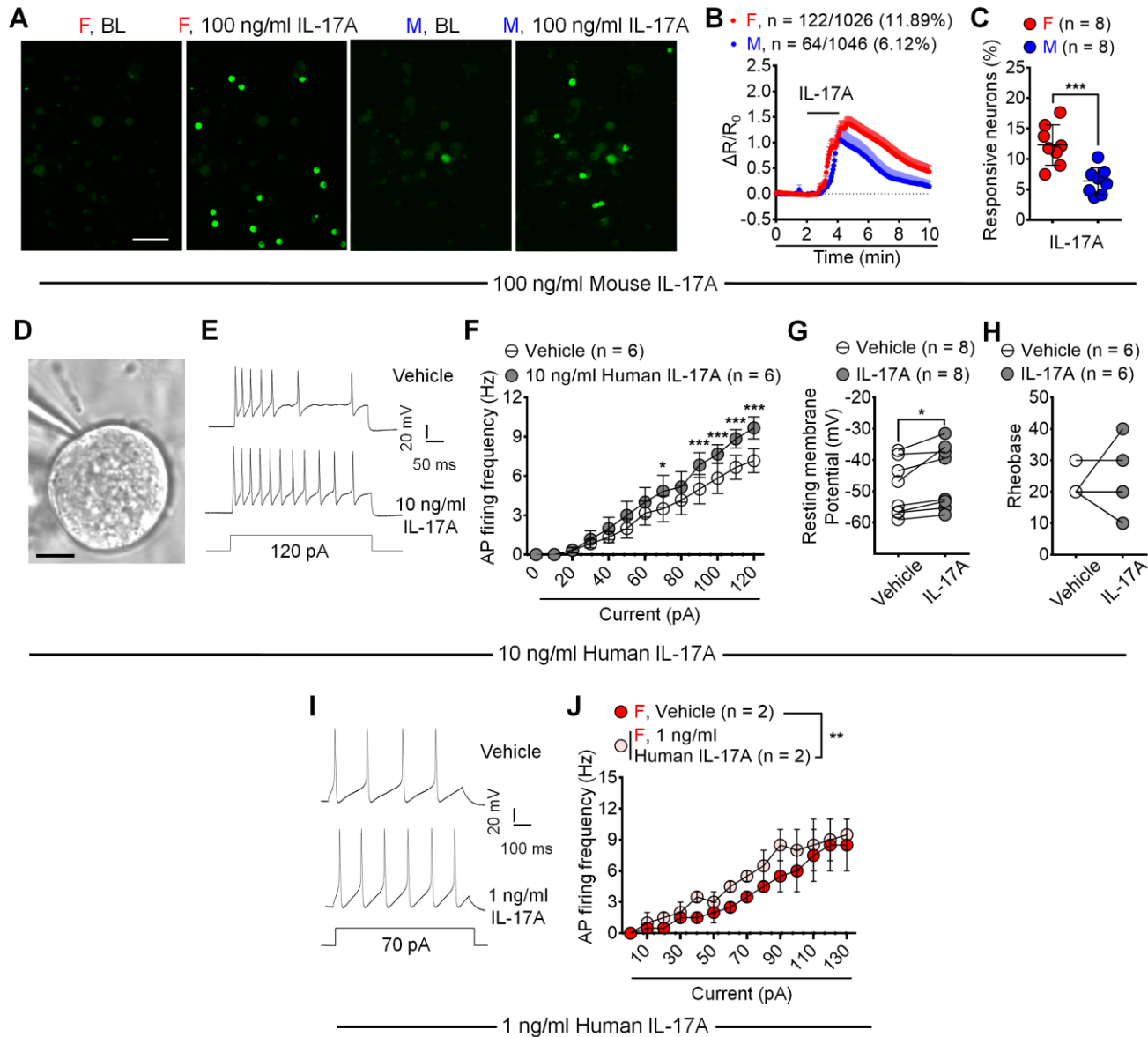


Figure S6 (related to Figure 6). IL-17A activates mouse and human DRG sensory neurons.

(A-C) Acute perfusion of IL-17A (100 ng/ml, 2 min) evokes Ca^{2+} influx in DRG sensory neurons cultured from both female and male *Advillin^{Cre}/GCamp6f* mice.

(A) Representative images. Scale bar: 100 μm .

(B) Combined responses of all neurons.

(C) % quantification of responding neurons. Notably, 11.89% of female neurons (122/1026) and 6.12% male neurons (64/1046) respond to IL-17A. n = 8 cultures from 4 mice per sex. Unpaired two-tailed student t test: p = 0.0009, t = 4.211.

(D-J) Responses of human DRG neurons to IL-17A.

(D) Representative image showing human DRG neuron being recorded. Scale bar: 20 μm .

(E) Traces of APs in human DRG neurons (from 2 male and 1 female donors) perfused with vehicle or IL-17A (10 ng/ml, 2 min).

(F) Quantification of AP firing frequencies as shown in (D). *p < 0.05, ***p < 0.001. Two-way RM ANOVA with Bonferroni's post hoc test; F (12, 60) = 36.45.

(G-H) Effects of IL-17A on resting membrane potential (G) and rheobase (H) of human DRG neurons. Paired and two-tailed Student's t-test; G: $t = 3.143$; H: $t = 0.0$.

(I-J) Acute perfusion of IL-17A (1 ng/ml, 2 min) increases SP firing in human DRG neurons from one female donor, as indicated by AP traces (I) and quantification of AP firing rate (J). $**p < 0.01$. Two-way RM ANOVA with Bonferroni's post hoc test; $F_{(13, 13)} = 5.939$.

Data are mean \pm SEM. AP: Action potential.

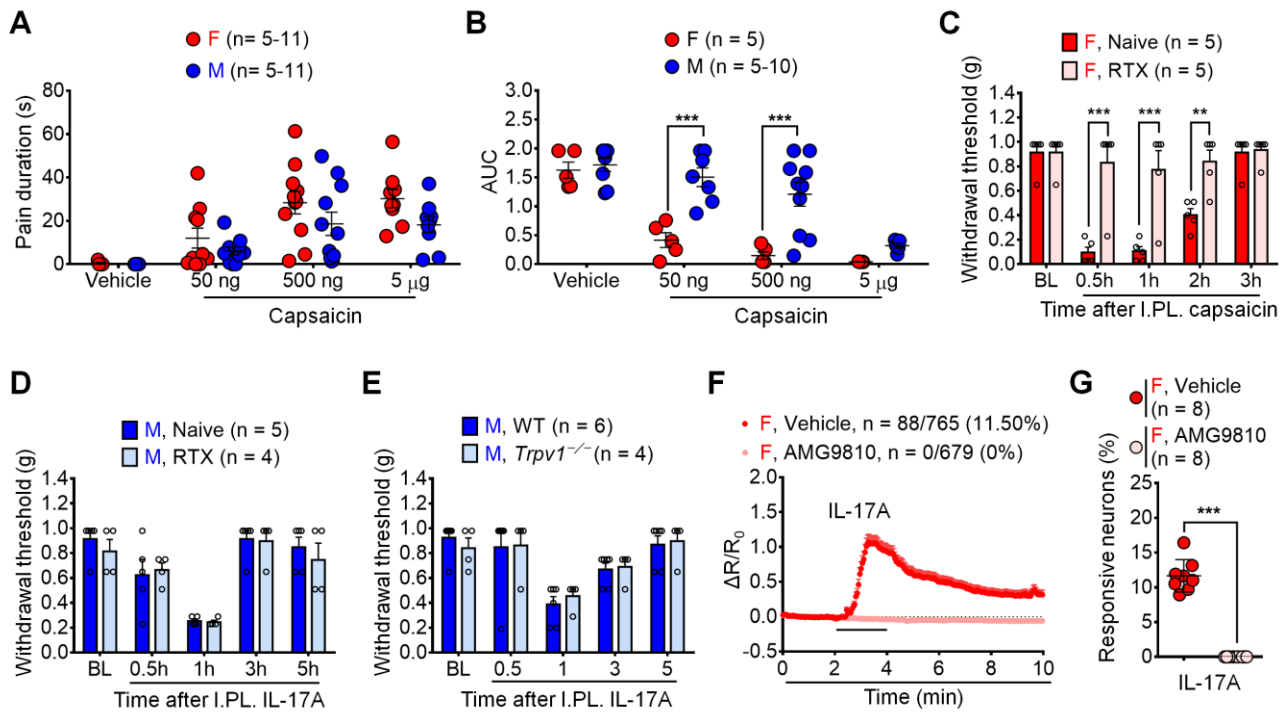


Figure S7 (related to Figure 7). IL-17A-induced pain does not require C-fiber nociceptors and TRPV1 in males.

(A) I.PL. injection of capsaicin at 50 ng, 500 ng or 5 μ g produces comparable spontaneous pain in both sexes. Two-way ordinary ANOVA with Bonferroni's post hoc test; $F_{(3, 62)} = 0.5063$. Note females show a trend of greater spontaneous pain than males.

(B) AUC of 0.5-2h data in Fig. 7E shows that capsaicin at 50 ng and 500 ng induces female-dominant mechanical pain. $***p < 0.001$. Two-way ordinary ANOVA with Bonferroni's post hoc; $F_{(3, 42)} = 5.227$

(C) RTX abolishes capsaicin-induced mechanical pain (I.PL., 500 ng) in females. $**p < 0.01$, $***p < 0.001$. Two-way RM ANOVA with Bonferroni's post hoc test; $F_{(4, 32)} = 6.777$. RTX was given by subcutaneous injections for 3 continuous days at the escalating doses of 30, 50 and 100 μ g/kg

(D-E) RTX treatment (D) or *Trpv1*^{-/-} (E) fails to reduce IL-17A-induced pain (I.PL., 100 ng) in males. Two-way ANOVA with Bonferroni's post hoc; D: $F_{(4, 28)} = 0.2786$; E: $F_{(4, 32)} = 0.2119$.

(F-G) Ca²⁺ response induced by IL-17A (100 ng/ml, 2 min) in dissociated DRG neurons and its blockade by the TRPV1 antagonist AMG9810 (3 μ M) in females.

(F) Combined responses of all neurons.

(G) % quantification of responding neurons. n = 8 cultures from 3 mice per group. Unpaired two-tailed student t test: $p < 0.0001$, $t = 14.12$.

Data are mean \pm SEM. AUC: Area under curve; RTX: Resiniferatoxin; I.PL.: Intraplantar; BL: Baseline.

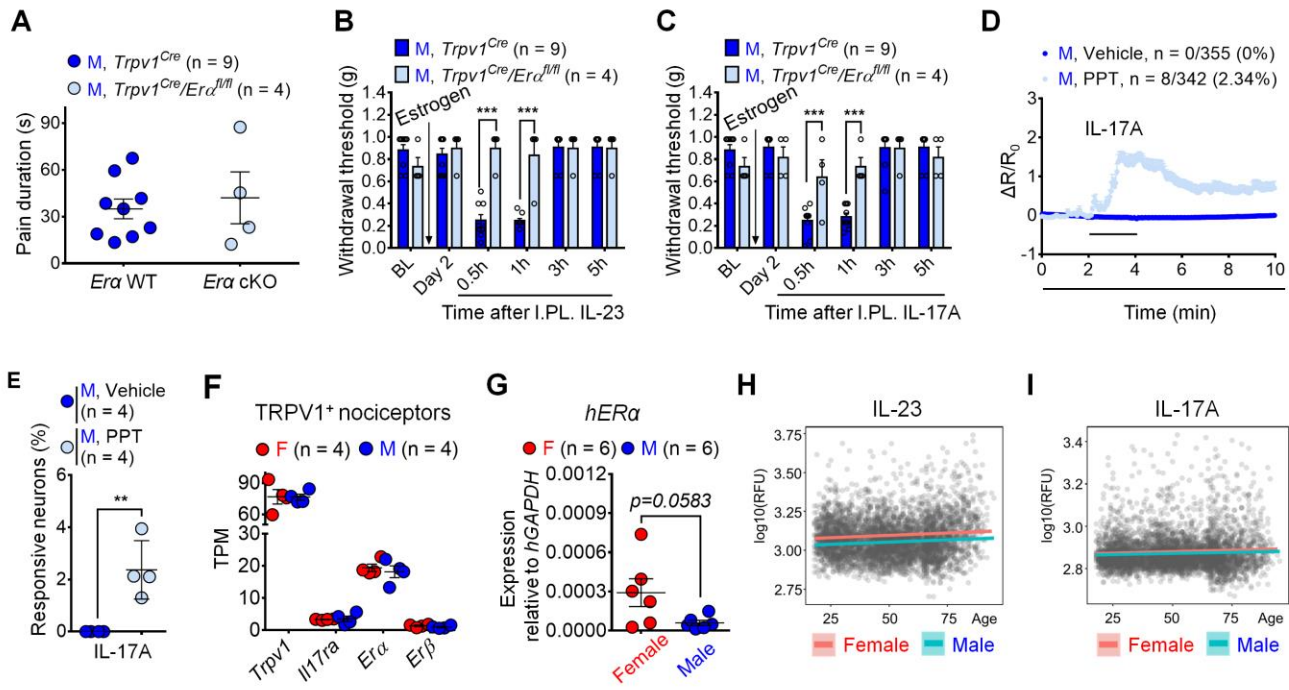


Figure S8 (related to Figure 8). Characterization of *Era* cKO in male mice and Translational relevance of IL-23/IL-17A/*ERα* axis in humans.

(A) Selective deletion of *Era* in nociceptors (*Era* cKO) fails to alter capsaicin-evoked spontaneous pain (I.PL., 500 ng) in males. Unpaired and two-tailed student t test; $t = 0.4973$.

(B-C) Estrogen treatment (S.C., 2 mg/kg) enables mechanical pain in male mice, induced by IL-23 (B, I.PL., 100 ng) or IL-17A (C, I.PL., 10 ng), which is abolished by *Era* cKO. *** $p < 0.001$. Two-way ANOVA with Bonferroni's post hoc test; B: $F_{(5, 55)} = 14.52$; C: $F_{(5, 55)} = 8.752$.

(D-E) IL-17A (10 ng/ml, 2 min) evokes Ca^{2+} influx in PPT (*ERα* agonist, 1 ng/ml, 24 h) incubated DRG neurons from male *Advillin^{Cre}/GCamp6f* mice.

(D) Combined responses of all neurons.

(E) % quantification of responding neurons. $n = 4$ cultures from 2 male mice. Unpaired two-tailed student t test; $p = 0.0055$, $t = 4.231$.

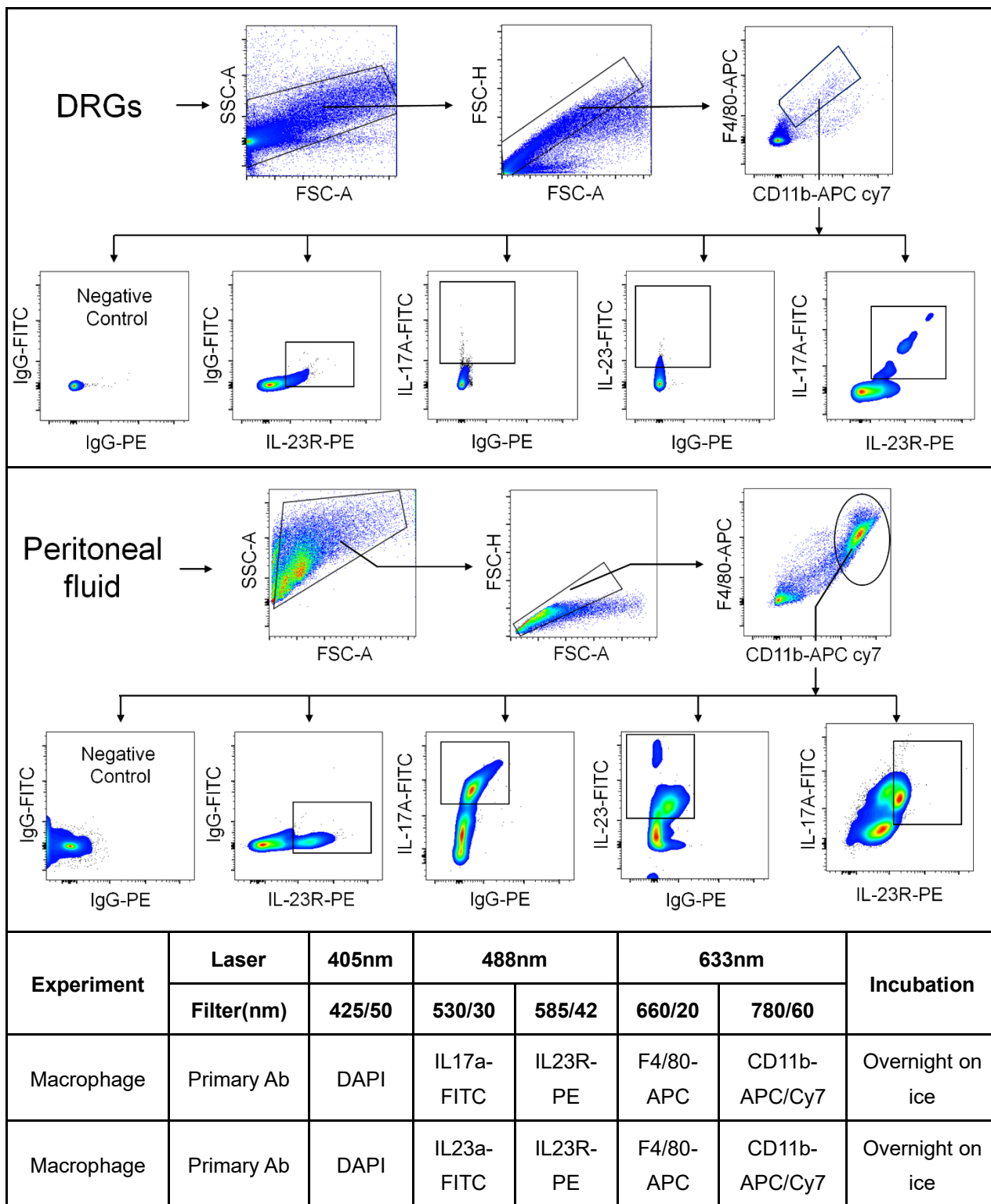
(F) Transcriptional profiles of mouse *Nav1.8⁺* C-fiber nociceptors reveal no sex differences in neuronal expression of *Trpv1*, *Il17ra*, *Era* and *Erβ* (Tavares-Ferreira et al. 2020). Two-way ordinary ANOVA with Bonferroni's post hoc test; $F_{(3, 24)} = 0.02263$.

(G) qPCR showing the expression of human *ERα* and *ERβ* mRNAs in DRGs using alternative primer pairs. Human *GAPDH* was used as an internal control. Unpaired and two-tailed student t test; $t = 2.137$. Also see primer information in Table S2.

(H-I) Healthy women ($n = 2,146$) display higher levels of IL-23 and IL-17A in plasma than healthy men ($n = 2,117$) throughout the life span (Lehallier et al. 2019).

Data are mean \pm SEM. cKO: Conditional knockout mice; TPM: Transcripts per million; S.C.: Subcutaneous; I.PL.: Intraplantar; ER: Estrogen receptor

Table S1 (related to Figures 4 and 5). Gating strategy and antibodies used for flow cytometry



Total cells from DRG or peritoneal fluid were first gated on a forward scatter (FSC-A) / side scatter (SSC-A) plot and then on the FSC-A/FSC-H (2×10^4 cells). The total macrophage population was gated on F4/80 and CD11b, in which IL-23⁺, IL-23R⁺, IL-17A⁺ and IL-17A⁺/IL-23R⁺ subsets were detected and analyzed.

Table S2 (related to Figure 8). qPCR primer sequences of human genes

TARGET GENE/SEQUENCE	APPLICATION	GENEBANK#
Primer: <i>hGAPDH</i> (Forward): AGCCACATCGCTCAGACAC	Figures 8I-8L, Figure S8G	NM_002046.7
Primer: <i>hGAPDH</i> (Reverse): GCCCAATACGACCAAATCC		
Primer: <i>hTPRV1</i> (Forward): CTGCCCCGACCATCACAGTC	Figure 8I	NM_080704.4
Primer: <i>hTPRV1</i> (Reverse): CTGCGATCATAGAGCCTGAGG		
Primer: <i>hIL17RA</i> (1) (Forward): GCTTCACCCTGTGGAACGAAT	Figure 8J	NM_014339.7
Primer: <i>hIL17RA</i> (1) (Reverse): TATGTGGTGCATGTGCTCAAA		
Primer: <i>hERα</i> (1) (Forward): GCTTACTGACCAACCTGGCAGA	Figure 8K	NM_000125.4
Primer: <i>hERα</i> (1) (Reverse): GGATCTCTAGCCAGGCACATTC		
Primer: <i>hERβ</i> (1) (Forward): AGCACGGCTCCATATACATACC	Figure 8L	NM_001291712.2
Primer: <i>hERβ</i> (1) (Reverse): TGGACCACTAAAGGAGAAAGGT		
Primer: <i>hERα</i> (2) (Forward): CCCACTCAACAGCGTGTCTC	Figure S8G	NM_000125.4
Primer: <i>hERα</i> (2) (Reverse): CGTCGATTATCTGAATTTGGCCT		

Table S3 (related to all figures). Number of animals used in all figures of this paper

Figure	Sample size	Number of groups	Sample size	Sex	Age (week)	Number of animals
1A	n = 5-9 mice	8	50	20 male, 30 female	8-10	50 WT mice
1B	n = 5-9 mice	8 (same mice with Figure 1A)	50	20 male, 30 female	8-10	50 WT mice
1C	n = 5-9 mice	8 (same mice with Figure 1A)	50	20 male, 30 female	8-10	50 WT mice
1D	n = 15 mice	2	30	30 female	8-10	15 WT mice, 15 <i>I23^{r/-}</i> mice
1E	n = 5 mice	2	10	10 male	8-10	10 WT mice
1H	n = 6-10 mice	4	33	14 male, 19 female	8-10	33 WT mice
1I	n = 5-10 mice	4	30	10 male, 20 female	8-10	30 WT mice
2A	n = 7 mice	4	28	14 male, 14 female	8-10	28 WT mice
2B	n = 7 mice	4 (same mice with Figure 2A)	28	14 male, 14 female	8-10	28 WT mice
2C	n = 9-10 mice	4	39	19 male, 20 female	8-10	20 WT mice, 19 <i>I23^{r/-}</i> mice
2D	n = 5 mice	4	20	10 male, 10 female	8-10	10 WT mice, 10 <i>I23^{r/-}</i> mice
2E	n = 6 mice	4	24	12 male, 12 female	8-10	24 WT mice
2F	n = 5-6 mice	4	22	12 male, 10 female	8-10	22 WT mice
2G	n = 5 mice	4	20	10 male, 10 female	8-10	20 WT mice
2H	n = 5 mice	4	20	10 male, 10 female	8-10	20 WT mice
2I	n = 5-7 mice	4	22	10 male, 12 female	8-10	22 WT mice
2J	n = 5-7 mice	4 (same mice with Figure 2I)	22	10 male, 12 female	8-10	22 WT mice
3A	n = 5 mice	2	10	10 female	8-10	10 WT mice
3B	n = 5 mice	6	30	30 male	8-10	30 WT mice
3C	n = 5 mice	2	10	10 female	8-10	10 WT mice
3D	n = 5 mice	2	10	10 male	8-10	10 WT mice
3E	n = 5 mice	2	10	10 female	8-10	10 WT mice
3F	n = 5 mice	2	10	10 male	8-10	10 WT mice
3G	n = 5 mice	4	10	10 male, 10 female	8-10	20 WT mice
4A	n = 6 mice	2	12	12 female	8-10	12 WT mice
4B	n = 6 cultures	4	24	12 male, 12 female	8-10	24 WT mice
4C	n = 5 mice	4	20	10 male, 10 female	8-10	20 WT mice
4D	n = 5 mice	4	20	10 male, 10 female	8-10	20 WT mice
4E	n = 5 mice	4	20	10 male, 10 female	8-10	20 WT mice
4F	n = 5-6 mice	4	21	21 female	8-10	11 Nude mice, 10 <i>Rag1^{-/-}</i> mice
4G	n = 5-9 mice	4	27	27 female	8-10	27 WT mice
4H	n = 5 mice	3	15	15 female	8-10	15 WT mice
4I	n = 5 mice	2	10	16 female	8-10	10 WT mice
4J,4K	n = 212-237 neurons; n = 6 cultures	2	-	3 male, 3 female	5-8	6 <i>Advillin^{Cre}/GCaMP6f</i> mice
4M	n = 7 neurons	2	-	3 female	5-8	3 WT mice
5A	n = 5 mice	8	40	20 male, 20 female	8-10	20 WT mice, 20 <i>I23^{r/-}</i> mice
5B	n = 7 cultures	4	28	14 male, 14 female	8-10	28 WT mice
5C	n = 5 mice	8	40	20 male, 20 female	8-10	40 WT mice
5D	n = 5 mice	8	40	20 male, 20 female	8-10	40 WT mice
5E	n = 5 mice	8 (same mice with Figure 5D)	40	20 male, 20 female	8-10	40 WT mice
5F	n = 5 mice	8 (same mice with Figure 5C)	40	20 male, 20 female	8-10	40 WT mice
5G	n = 8 mice	3	24	24 female	8-10	24 WT mice
5H	n = 6 mice	2	12	12 female	8-10	12 WT mice
5I	n = 6 mice	2	12	12 female	8-10	6 WT mice, 6 <i>I23^{r/-}</i> mice
5J	n = 5 mice	2	10	10 female	8-10	10 WT mice

5K	n = 5 mice	2	10	10 male	8-10	10 WT mice
5L	n = 6 mice	4	24	12 male, 12 female	8-10	24 WT mice
5M	n = 6 mice	4	24	12 male, 12 female	8-10	24 WT mice
6B,6C	n = 717-1209 neurons; n = 8 – 12 cultures	2	-	4 male, 4 female	4-6	8 <i>Advillin^{Cre}/GCaMP6f</i> mice
6E	n = 7 neurons	2	-	3 female	8-10	3 WT mice
6G	n = 9 neurons	2	-	3 male	8-10	3 WT mice
6I	n = 9 neurons	2	-	2 female	-	2 NHP
6K	n = 8 neurons	2	-	1 male	-	1 NHP
7A	n = 5-8 mice	4	27	27 female	8-10	27 <i>Trpv1^{-/-}</i> mice
7B	n = 5 mice	4 (same female mice with Figure 7A)	20	10 male, 10 female	8-10	20 <i>Trpv1^{-/-}</i> mice
7C	n = 5 mice	4	20	20 female	8-10	20 <i>Trpa1^{-/-}</i> mice
7D	n = 4-5 mice	4 (same female mice with Figure 7C)	19	9 male, 10 female	8-10	19 <i>Trpa1^{-/-}</i> mice
7E	n = 5-10 mice	8	50	30 male, 20 female	8-10	50 WT mice
7F	n = 5 mice	2 (same mice with Figure 5H)	10	10 female	8-10	10 WT mice
7G	n = 5 mice	2 (same mice with Figure 5I)	10	10 male	8-10	10 WT mice
7I	n = 4 mice	2	8	4 male, 4 female	8-10	8 WT mice
7J	n = 4 mice	2 (same mice with Figure 7M)	8	4 male, 4 female	8-10	8 WT mice
7K	n = 4 mice	2 (same mice with Figure 7M)	8	4 male, 4 female	8-10	8 WT mice
7L	n = 5 mice	2	10	10 female	8-10	10 WT mice
7M	n = 6 mice	2	12	12 female	8-10	6 WT mice, 6 <i>Trpv1^{-/-}</i> mice
7N,7O	n = 278 – 623 neurons; n = 4 – 6 cultures	2	-	2 female	8-10	2 <i>Advillin^{Cre}/GCaMP6f</i> mice
7P	n = 8 neurons	2	-	3 female	8-10	3 <i>Trpv1^{-/-}</i> mice
8B	n = 4 mice	2 (same mice with Figure 7M)	8	4 male, 4 female	8-10	8 WT mice
8C	n = 4 mice	2 (same mice with Figure 7M)	8	4 male, 4 female	8-10	8 WT mice
8D	n = 16 slides / 4 mice	2 (same mice with Figure 7M)	-	4 male, 4 female	8-10	8 WT mice
8E	n = 9-10 mice	2	19	19 female	8-10	10 <i>Trpv1^{Cre}</i> mice, 9 <i>Trpv1^{Cre}/Era^{fl/fl}</i> mice
8F	n = 9-10 mice	2 (same mice with Figure 8E)	19	19 female	8-10	10 <i>Trpv1^{Cre}</i> mice, 9 <i>Trpv1^{Cre}/Era^{fl/fl}</i> mice e
8G	n = 9-10 mice	2 (same mice with Figure 8E)	19	19 female	8-10	10 <i>Trpv1^{Cre}</i> mice, 9 <i>Trpv1^{Cre}/Era^{fl/fl}</i> mice
8H	n = 8-9 mice	2 (same mice with Figure 8E)	17	17 female	8-10	9 <i>Trpv1^{Cre}</i> mice, 8 <i>Trpv1^{Cre}/Era^{fl/fl}</i> mice
S1A	n = 5-9 mice	8 (same mice with Figure 1A)	50	20 male, 30 female	8-10	50 WT mice
S1B	n = 5 mice	8	40	20 male, 20 female	8-10	40 WT mice
S2A	n = 4-5 mice	4 (same mice with Figure 2C)	19	9 male, 10 female	8-10	10 WT mice, 9 <i>Il23^{-/-}</i> mice
S2B	n = 5 mice	4 (same mice with Figure 2D)	20	10 male, 10 female	8-10	10 WT mice, 10 <i>Il23^{-/-}</i> mice
S3A	n = 5 mice	2 (same mice with Figure 3G)	10	10 female	8-10	10 WT mice
S3B	n = 5 mice	2 (same mice with Figure 3G)	10	10 male	8-10	10 WT mice
S3C	n = 5 mice	4	20	10 male, 10 female	8-10	20 WT mice
S3D	n = 5 mice	4 (same mice with Figure S3C)	20	10 male, 10 female	8-10	20 WT mice
S4B	n = 8-9 mice	4	34	16 male, 18 female	8-10	34 WT mice
S4D	n = 14-17 mice	4	61	29 male, 32 female	8-10	61 WT mice
S4F	n = 6 cultures	4	24	12 male, 12 female	8-10	24 WT mice
S4H	n = 8-15 cultures	4	45	20 male, 25 female	8-10	45 WT mice
S5B	n = 11-13 mice	4	48	22 male, 26 female	8-10	48 WT mice
S5D	n = 11-13 mice	4	46	22 male, 24 female	8-10	46 WT mice
S5F	n = 8 cultures	4	32	16 male, 16 female	8-10	32 WT mice
S5H	n = 8-15 culture	4	43	20 male, 23 female	8-10	45 WT mice
S6B	n = 1026-1046 neurons n = 8 cultures	2 (same mice with Figure 6B)	3	4 male, 4 female	8-10	8 <i>Advillin^{Cre}/GCaMP6f</i> mice

S7A	n = 5-11 mice	8	66	33 male, 33 female	8-10	66 WT mice
S7B	n = 5-10 mice	8 (same mice with Figure 7E)	50	30 male, 20 female	8-10	50 WT mice
S7C	n = 5 mice	2	10	10 female	8-10	10 WT mice
S7D	n = 4-5 mice	2	9	9 male	8-10	9 WT mice
S7E	n = 4-6 mice	2	10	10 male	8-10	6 WT mice, 4 <i>Trpv^{-/-}</i> mice
S7F,7G	n = 679-765 neurons n = 8 cultures	2	-	3 female	8-10	3 <i>Advillin^{Cre}/GCaMP6f</i> mice
S8A	n = 4-9 mice	2	13	13 male	8-10	9 <i>Trpv1^{Cre}</i> mice, 4 <i>Trpv1^{Cre}/Erg^{fl/fl}</i> mice
S8B	n = 4-9 mice	2 (same mice with Figure S8A)	13	13 male	8-10	9 <i>Trpv1^{Cre}</i> mice, 4 <i>Trpv1^{Cre}/Erg^{fl/fl}</i> mice
S8C	n = 4-9 mice	2 (same mice with Figure S8A)	13	13 male	8-10	9 <i>Trpv1^{Cre}</i> mice, 4 <i>Trpv1^{Cre}/Erg^{fl/fl}</i> mice
S8D,E	n = 342-355 neurons n = 4 cultures	2	2	2 male	8-10	2 <i>Advillin^{Cre}/GCaMP6f</i> mice
Total # of mice						1586 (678 male + 908 female)
Total # of NHP						3 (1 male + 2 female)